

# RSC Advances



This is an *Accepted Manuscript*, which has been through the Royal Society of Chemistry peer review process and has been accepted for publication.

*Accepted Manuscripts* are published online shortly after acceptance, before technical editing, formatting and proof reading. Using this free service, authors can make their results available to the community, in citable form, before we publish the edited article. This *Accepted Manuscript* will be replaced by the edited, formatted and paginated article as soon as this is available.

You can find more information about *Accepted Manuscripts* in the [Information for Authors](#).

Please note that technical editing may introduce minor changes to the text and/or graphics, which may alter content. The journal's standard [Terms & Conditions](#) and the [Ethical guidelines](#) still apply. In no event shall the Royal Society of Chemistry be held responsible for any errors or omissions in this *Accepted Manuscript* or any consequences arising from the use of any information it contains.

Cite this: DOI: 10.1039/c0xx00000x

www.rsc.org/xxxxxx

## ARTICLE TYPE

**Cadmium selenide quantum dots to ameliorate the properties of a room temperature discotic liquid crystalline material**Neelam Yadav<sup>a</sup>, Sandeep Kumar<sup>b</sup> and Ravindra Dhar<sup>a\*</sup><sup>a</sup>Centre of Material Sciences, University of Allahabad, Allahabad 211002, India<sup>b</sup>Raman Research Institute, C.V. Raman Avenue, Sadashivanagar, Bangalore, India-560080.

10 Received (in XXX, XXX) Xth XXXXXXXXX 20XX, Accepted Xth XXXXXXXXX 20XX

DOI: 10.1039/b000000x

The effect of cadmium selenide quantum dots on a room temperature discotic liquid crystalline material has been studied. These composites were characterized using differential scanning calorimetry, polarizing optical microscopy, impedance spectroscopy and small angle X-Ray scattering. It was found that the composite with lowest concentration of quantum dots enhance the quasi one-dimensional conductivity by five orders of magnitude of the discotic liquid crystal without altering the columnar hexagonal phase. X-Ray scattering results reveal that a decrement in core-core distance is brought about by the intercalation of quantum dots in between columns of discotic liquid crystal matrix. Dielectric spectroscopy demonstrates a relaxation mode in the high frequency region of the pure discotic material as well as in the composites.

**Keywords:** anthraquinone derivatives, conductivity, relaxation frequency and dielectric strength.

\*Author for correspondence (email: dr\_ravindra\_dhar@hotmail.com)

## 1. Introduction

The 1, 2, 3, 5, 6, 7-hexahydroxy-9, 10-anthraquinone, generally called as rufigallol is known to act as a core fragment in variety of discotic liquid crystals (DLCs).<sup>1</sup> DLCs are self-assembled materials where noncovalent intermolecular interactions drive its self-assembly.<sup>2</sup> Rufigallol derivatives made of disc shaped molecules consist of an elongated core with a twofold symmetry axis which is substituted by flexible aliphatic side chains. These side chains lead to enhanced solubility, processability, and rich thermotropic behavior.<sup>3</sup> Furthermore, because of their liquid-character, they possess the capacity to self-heal structural defects such as grain boundaries.<sup>4</sup> They are one of the primitive systems to flaunt columnar mesophases.<sup>5, 6</sup> Columnar hexagonal phase exhibited by most of the rufigallol derivatives have strong anisotropic electronic transport properties that are related to unidirectional intermolecular coupling along the column axis.<sup>7, 8</sup> Shape anisotropy, micro segregation between rigid core and flexible chains and core-core Van der Waal attractions are the driving forces for the formation of columnar hexagonal mesophases. These smart materials show polymorphism, have high diffusion lengths, are thermally stable and

colored. These characteristics makes them promising candidates for applications in molecular electronics and high efficiency photoconductive switches, solar cells and organic light emitting diodes.<sup>9, 10</sup> However, the conductivity of these LCs is low. Doping them with nanomaterials can help in increasing their conductivity and making them more viable for use in technological applications.<sup>11</sup>

Merging the interesting self-organizing propensity of these rufigallol derivatives with the exceptional, readily tailored features of zero dimensional nanomaterials such as quantum dots (QDs) can be a challenging work and useful from application point of view. The three dimensional quantum confinement effect i.e. the strong confinement of electrons and holes where the radius of a particle is below the exciton Bohr radius of the material is responsible for their unique size and shape dependent electronic properties differing from the bulk counterparts.<sup>12, 13</sup> Their band gap is tunable to different wavelengths of light, allowing them to harness energy from the visible to the infrared regions. Their photochemical stability and small size makes them viable for manufacturing novel biological sensors, lasers,

resonators, and photovoltaic solar cells.<sup>14-17</sup> Kumar and co-workers presented data on DLC nanocomposites which show that QDs increase the electrical conductivity of the DLC host by two orders of magnitude.<sup>18</sup> Basu *et al.* demonstrated the formation of one dimensional chain like arrays and larger dielectric constant by doping CdS QD in nematic LC.<sup>19</sup> Biradar *et al.* achieved good memory effect by tuning CdTe QDs in ferroelectric LC that can be utilized in future zero power displays.<sup>20</sup> Hegmann and coworkers have worked extensively on LC nanocomposites and reported beneficial effects.<sup>21, 22</sup>

In this report, we use 1,5-dihydroxy-2,3,6,7-tetrakis(3,7-dimethyloctyloxy)-9,10-anthraquinone (RTAQ) as a host to incorporate CdSe QDs. RTAQ has the widest columnar hexagonal room temperature mesophase and is a difunctional molecule. Dielectric properties of DLCs in general and RTAQ in particular are least understood. Frequency and temperature dependent dielectric spectroscopy of RTAQ is not yet reported. In the present work, we have carried our dielectric spectroscopy on RTAQ and its composite with CdSe QDs. Our aim is to see how various dielectric parameters such as permittivity, conductivity, relaxation frequency (if any mode exists) and its strength are affected in the presence of QDs. These DLC+QDs composites may potentially possess versatile applications in electronic and optical nano-devices.

## 2. Experimental details

### 2.1. Materials

RTAQ molecule has two hydrogen bonds. It is deep orange in color. It was synthesized in the same manner as reported earlier by Kumar *et al.*<sup>23</sup> It shows a columnar hexagonal phase confirmed by X-Ray diffraction studies as well as POM.<sup>51</sup> CdSe QDs essentially are mono disperse and have an average diameter of 3.5 nm. They are highly soluble in non-polar solvents such as hexane, toluene, and chloroform. Details on the preparation and the characterization of the CdSe nanoparticles have been described elsewhere.<sup>24, 25</sup>

### 2.2. Preparation of composites

To prepare the composites, a solution of CdSe QDs in chloroform was added to a previously weighed RTAQ placed in a vial. The contents of the vial were subjected to ultrasonication for five hours to ensure uniform dispersion. The chloroform was evaporated slowly (within ~24 hours) leaving behind the RTAQ+QDs mixture. However, before taking the material for various measurements, it is once again mixed in its isotropic liquid phase (for about 30 minutes) with the help of magnetic stirrer. This process was repeated to prepare three composites viz., 0.5QDAQ, 1QDAQ, and 5QDAQ having 0.5 wt %, 1 wt % and 5 wt % QDs respectively, in RTAQ.

### 2.3. Sample Characterization

The differential scanning calorimetry measurements were performed on pure and dispersed samples with the help of

differential scanning calorimeter (DSC) of NETZSCH model DSC-200-F3-Maia. Peak transition temperature ( $T_p$  in °C) and associated transition enthalpy ( $\Delta H$  in J g<sup>-1</sup>) for various transitions were measured from -30°C to isotropic temperatures at scanning rates of 15, 12.5, 10, 7.5 and 5 °C min<sup>-1</sup> during the heating and cooling cycles. Polarised optical microscopy (POM) images were taken using polarized microscope coupled with an Instec MK 1000 heating stage. The dielectric studies of the samples were carried out under homeotropic geometry wherein plane of discotic molecules is parallel to the electrode's surfaces. The sandwiched type (capacitors) cells were made using two glass substrates coated with indium tin oxide (ITO) layers. The thickness of the cell was defined by placing two Mylar spacers (thickness 10 μm) between the glass plates. These cells have been used for the optical textures studies as well. The samples were introduced via capillary action by heating to the isotropic liquid phase. In order to achieve homeotropic alignment, the samples were slowly cooled at the rate of 0.1 °C-min<sup>-1</sup> from the isotropic phase without any chemical treatment. This usually adopted process yields reasonably good quality of homeotropic alignment due to minimum energy configuration of discotic molecules. For all POM imaging and electrical measurements, the LC mixtures were heated above the phase transition temperature and cooled at a rate of 0.1°C min<sup>-1</sup>. The temperature of the sample has been controlled with the help of a hot stage (Instec model HCS 302) joined with a temperature controller (Instec model mK 1000). The sample temperature has been determined by measuring thermo-emf of a copper-constantan thermocouple with the help of a six and half-digit multi meter from Agilent (model-34410A) with the accuracy of ±0.1°C. Dielectric data have been acquired by using the Newton's Phase Sensitive Multi meter (model-1735) coupled with IAI (model-1257) in the frequency range of 1Hz to 35 MHz. A measuring electric field of magnitude 500 mV<sub>rms</sub> was applied normal to electrode surfaces while acquiring the electrical data. POM and dielectric studies have been carried out during the cooling cycles where better alignment is expected than in the heating cycle. Detailed methodology and necessary mathematical equations to obtain the permittivity ( $\epsilon'$ ), loss ( $\epsilon''$ ) and conductivity ( $\sigma$ ) of the materials is reported elsewhere.<sup>26, 27</sup> Small angle X-ray scattering (SAXS) studies were carried out using an X-ray diffractometer (Rigaku, UltraX 18) operating at 50 kV and 80 mA current having Cu-K $\alpha$  radiation of the wavelength of 1.54 Å.

## 3. Results and Discussion

### 3.1 DSC studies

The mesophase behavior of pure RTAQ and composites has been studied by DSC. Fig. 1 presents the DSC thermograms taken during heating and cooling at the scan rate of 5 °C/min. for pure RTAQ and three composites. The pure sample and composites on heating and cooling

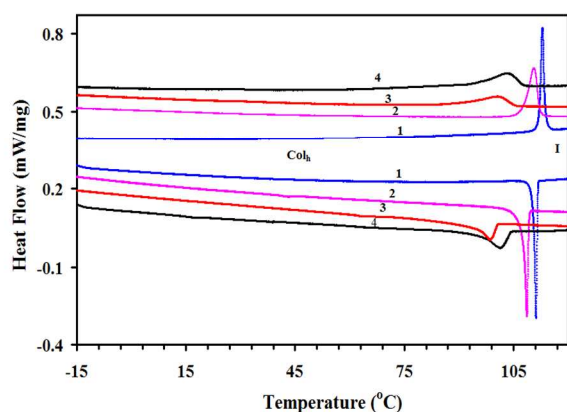


Figure 1: DSC curves taken during heating and cooling for (1) Pure RTAQ (2) 0.5QDAQ (3) 1QDAQ and (4) 5QDAQ.

show peaks signifying columnar hexagonal-isotropic (Col<sub>h</sub>-I) and isotropic-columnar hexagonal (I-Col<sub>h</sub>) transitions respectively. In general, these two transitions are expected at the same temperature under the condition of thermodynamic equilibrium. However, in the case of the dynamic process (scan rate 5.0 °C/min), thermodynamic equilibrium is not achieved and hence these two transitions occur at different temperatures. During the heating cycle, detected transition temperature is higher whereas during the cooling it is lower than the actual transition temperature. As scan rate increases, system moves away from the condition of thermodynamic equilibrium due to thermal inertia and hence above difference increases.<sup>28,29</sup> It has been observed that transition temperatures vary linearly with the scanning rate with opposite slopes in the heating (positive) and cooling (negative) cycles as reported earlier also.<sup>28,29</sup> However, extrapolated transition temperatures at the (hypothetical) scanning rate of 0 °C/min agree for the heating and cooling cycles of the enantiotropic phase transitions except when there is some super cooling effect.<sup>28,29</sup> Extrapolated transition temperatures thus obtained are given in Table-1 and are same for Col<sub>h</sub>-I and I-Col<sub>h</sub> transitions. Thus Col<sub>h</sub>-I and I-Col<sub>h</sub> transitions are equivalent and hence forth we will call it I-Col<sub>h</sub> transition as most of the other experiments have been performed during the cooling cycle. A significant effect observed is the decrease of the I-Col<sub>h</sub> transition temperatures for the composites (see Table 1) as compared to the pure sample; the effect becomes more pronounced as the concentration of QDs is increased. This is expected to be arising as an impurity effect, since QDs in the composites are non-liquid crystalline component. QDs tend to intercalate between the columns, weakening the inter columnar interaction. However, another interesting result obtained for 0.5QDAQ is that the enthalpy of this transition (refer Table 1) increases by 17% as compared

40 Table 1: Transition temperatures ( $T_{I-Col_h}$  in °C) obtained from DSC as well as POM and dielectric studies, corresponding enthalpies ( $\Delta H$  in J g<sup>-1</sup>) obtained from DSC, relaxation frequency ( $f_R$  in kHz), and strength of relaxation mode ( $\delta\epsilon$ ) obtained by fitting dielectric spectra to eq. 3 at 30.5 °C for pure and composite systems.

System	$T_{I-Col_h}$		$\Delta H$	$f_R$	$\delta\epsilon$
	DSC	POM/ Dielectric Studies			
RTAQ	112.2	112.4	5.8	408	1.12
0.5QDAQ	110.1	110.6	6.8	394	1.12
1QDAQ	99.4	99.6	4.2	359	1.11
5QDAQ	102.5	102.8	4.8	363	0.97

to pure RTAQ which indicates that stability of the Col<sub>h</sub> has enhanced in the case of 0.5QDAQ. Also, the peak for the Col<sub>h</sub>-I/ I-Col<sub>h</sub> transition is almost symmetric as in the case of pure RTAQ. At the clearing temperature, unstacking of molecular cores takes place. When concentration is low, QDs are adjusted between flexible chains and resist unstacking of molecular cores. All these suggest that the ordering of molecular discs inside a column increases. For 1QDAQ and 5QDAQ, peaks become highly asymmetric with decrease of height by 90% and 88% respectively (with respect to pure sample) indicating that higher concentration of QDs slows down the transition process. Here it is important to point out that peak height represents maximum of rate of heat flow with time. When the concentration of QDs is increased above 0.5 wt%, they tend to disrupt the columns and induce defects in it. Large size of the aggregated QDs disturbs the packing of the molecular discs as they cannot be adjusted between flexible chains without disturbing columns. This leads to decrease in enthalpy of the Col<sub>h</sub>-I transition. On the basis of thermodynamic results, we have indication that the low concentration of QDs (0.5 wt %) is uniformly miscible with RTAQ but as concentration increases, miscibility decreases. This result is in conformation with those obtained from optical microscopic and dielectric studies discussed in the forthcoming sections. Immiscibility and phase separation at higher concentrations has been reported by the other workers as well.<sup>30</sup> As long as there is good miscibility, QDs act as impurity and I-Col<sub>h</sub> transition temperature decreases according to general rule. With the increasing concentration of QDs, when miscibility becomes poor (5 wt %), there seems phase separation like behavior and I-Col<sub>h</sub> transition temperature tries to return towards the original value of RTAQ.

### 3.2. Optical studies

POM under crossed polarizer condition is used to image the spatial variation in director orientation, as LCs are

optically anisotropic. Phase transitions for all the samples are clearly visible under POM. I-Col<sub>h</sub> transition temperatures obtained from POM are slightly higher than those obtained from DSC (see table 1). This is because transition temperatures obtained from DSC are peak temperatures (where process of transition is maximum) whereas in the case of POM studies, these are onset (i.e. start of transition) temperatures. Environment around the sample is also different in two cases. In the case of DSC, sample is under the inert atmosphere whereas in the case of POM it is under normal atmosphere. The colour and area

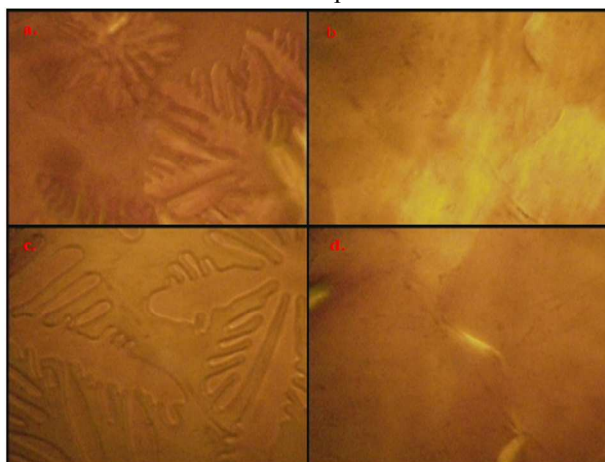


Figure 2: POM images (a) for pure RTAQ at 112.4°C while transition (b) for pure RTAQ at 49.1°C in complete Col<sub>h</sub> phase (c) for 0.5QDAQ at 110.6°C while transition (d) for 0.5QDAQ at 68.9°C in complete Col<sub>h</sub> phase.

of the domains changes with temperature also. Figs. 2a-b show optical textures of pure RTAQ. These textures reveal some dark areas which show that the columns get easily aligned homeotropically (i.e. column axis is perpendicular to glass substrates) on untreated glass substrates when cooled slowly i.e. at rate of 0.1 °C/min from the isotropic

phase.<sup>31</sup> Some bright domains can also be seen which indicate areas where molecular planes may be minutely tilted with respect to substrates. These are  $\pi$  disclinations or defects.<sup>32</sup> POM images of 0.5QDAQ are shown in figs 2c-d. Here entire field of view became dark when the sample is in complete mesophase (fig 2d). This suggests that addition of QDs leads to the decrease in  $\pi$  disclinations or defects. QDs help to align the disk shaped molecules inside a column, leading to better homeotropic arrangement of columns on the glass substrates. It is known that rigid cores of discotic molecules are translationally disordered within columns.<sup>33</sup> Microscopic observations on 1QDAQ (shown in figs. 3a-d) represent increased number of  $\pi$  disclinations like regions. This shows that as concentration of QDs is increased, they tend to tilt the molecular disks inside a column slightly. Prasad *et al.* have previously described such textures of columnar hexagonal phase of a novel series of anthraquinone based DLC with bulky substituent.<sup>32</sup> Highly bright textures were observed for 5QDAQ as shown in figs. 3e-h which is completely distinct from those in figs. 3a-d. While cooling in columnar phase, textures show continuous changes with the appearance of defect like regions. Large domains increase in size while cooling from the isotropic phase at about 84.3 °C. On further cooling at about 82.6 °C (see fig. 3g), number of defects appear on domain and tend to rise with cooling. Aggregation of QDs may lead to development of such defects in DLC. Several reports state that after a certain concentration, nanoparticles have a tendency to aggregate.<sup>34</sup> Kinkead and Hegmann have also reported tendency of CdSe QDs to aggregate above 1 wt% when doped in a nematic liquid crystal.<sup>21</sup> However; aggregates that may eventually form at the higher concentration are not directly visible at magnifications up to 100x. There is no sign of crystallization in case of pure and composites while cooling the samples to the room temperature which confirms the results obtained from DSC.

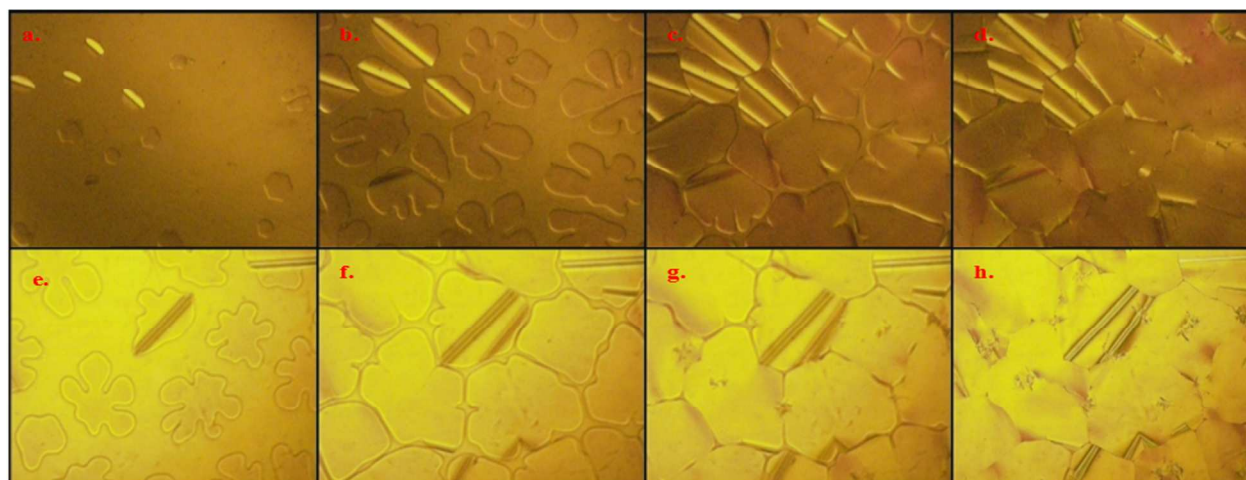


Figure 3(a-d) POM images taken while cooling for 1QDAQ (a) at transition 99.3°C (b) at 88.2°C (c) at 82.6°C and (d) 30.5°C in complete Col<sub>h</sub> phase. (e-f) for 5QDAQ (e) at transition 102.8°C (f) 84.3°C (here in each domains columns are aligned unidirectional) (g) 82.6°C (one can note here appearance of defects on domains) and (h) at 30.5°C where defects are further dominated.

Cite this: DOI: 10.1039/c0xx00000x

www.rsc.org/xxxxxx

## ARTICLE TYPE

## 3.3. Dielectric studies

Conductivity measurements were carried out on pure RTAQ and its composites to evaluate the effect of QDs dispersion on the electrical properties of DLC. Fig. 4 shows the temperature variation of DC conductivity for pure and composites. The conductivity of virgin RTAQ is of the order of  $10^{-10}$  S-m<sup>-1</sup>. Enhancement in conductivity is observed by five orders of magnitude in the case of lowest concentration i.e. 0.5 wt% QDs in pure DLC. Conductivity

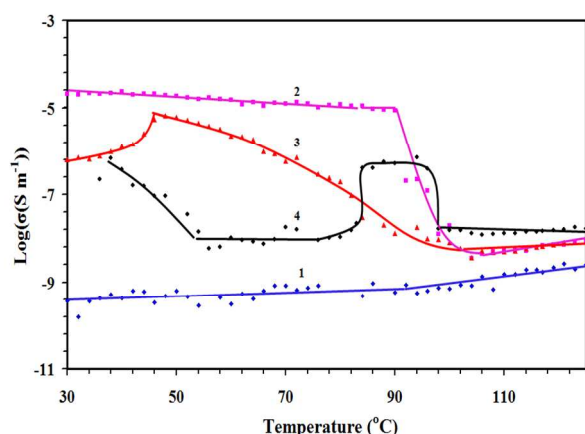


Figure 4: Temperature dependence of DC conductivity : Curve (1) Pure RTAQ (2) 0.5QDAQ (3)1QDAQ and (4)5QDAQ. The lines are guide to the eyes.

of 0.5QDAQ has been found to be  $6 \times 10^{-9}$  S-m<sup>-1</sup> in the isotropic phase. It increases with decrease in temperature, becoming  $8.95 \times 10^{-6}$  S-m<sup>-1</sup> at 86.2 °C and finally reaching to a value of  $2.05 \times 10^{-5}$  S-m<sup>-1</sup> at 30.5 °C. The drastic increment in conductivity can be attributed to the ordered arrangement of discotic molecules and QDs as evidenced by the optical texture (see fig 2d) discussed in the previous section. Based on Marcus equation, the theoretical description of electron hopping rate between adjacent discs is explained by the transfer integral which is a function of LUMO (HOMO) orbitals of adjacent molecules for electron (hole) transport and internal reorganization energy.<sup>35</sup> Charge transport in the bulk material depends on the degree of order within the columnar stack and thus on the overlap between the  $\pi$ -orbitals.<sup>36</sup> Chandrashekhar *et al.* have asserted that the rigid core of DLCs are ordered, orientational order parameter  $S$ , defined as ( $S = \langle \frac{1}{2}(3\cos^2\theta - 1) \rangle$ ), where,  $\theta$ = angle which molecular symmetry axis makes with director or column axis.<sup>37</sup> The core is not normal to column axis but is inclined in columnar mesophases. It is established that tilt of molecular core persists in columnar hexagonal phase as

well.<sup>38</sup> Also, mobility is dependent on intracolumnar order more than that on intercolumnar ordering.<sup>39</sup> Based on these facts, it can be inferred that the increase in the orientational order of rigid cores arises from the doping of QDs in DLC matrix. The overlapping of the  $\pi$ -orbitals of cores increases which in turn leads to increase in mobility along the columns. The QDs act as conductive filler which bridges the defects within the columnar matrix. Thus, high mobility along columns leads to very high conductivity for 0.5QDAQ. These experiments were repeated in order to validate the results obtained. X-ray diffraction studies (discussed in the forthcoming section) also explain increase in conductivity.

When the concentration of QDs in DLC is increased, the conductivity tends to decrease with respect to 0.5QDAQ. For 1QDAQ; conductivity is of the order of  $10^{-9}$  S-m<sup>-1</sup> in the isotropic liquid phase, it increases to  $2.0 \times 10^{-7}$  S-m<sup>-1</sup> at 78.3 °C and  $1.28 \times 10^{-6}$  S-m<sup>-1</sup> at 39.4 °C. In the case of 5QDAQ, conductivity increases from  $1.32 \times 10^{-9}$  S-m<sup>-1</sup> at 114.0 °C (Isotropic liquid phase), reaching a maximum of  $4.07 \times 10^{-7}$  S-m<sup>-1</sup> at 84.3 °C. At 82.6 °C, it abruptly decreases to  $2.18 \times 10^{-8}$  S-m<sup>-1</sup> and continues to do so till 60.0 °C. It is important to note that this is the same temperature where optical textures also show growth of some defects (refer fig. 3g). On further cooling, it shows an increasing trend. In this case when material is transferred to columnar mesophase (from isotropic liquid phase), initially conductivity is high when alignment is good. However, when temperature further decreases, perhaps due to aggregation of QDs, alignment deteriorates and hence conductivity decreases. Again when settlement of the discs improves with decrease in temperature, conductivity slowly increases. Such competition may occur during the whole cooling process. In other words, it is apparent that columns of the mesophase are not properly ordered (unidirectional) when aggregation occurs. This tendency increases with increase in the concentration of QDs leading to creation of more defects. Further, due to aggregation of QDs, the DLC takes time to settle down properly in its mesophase as revealed by POM and DSC. This also causes asymmetry of I-Col<sub>h</sub> peaks observed by DSC. Results obtained by Wood *et al.* also illustrate that colloidal particles incorporated in LCs decrease orientational order, generating defect lines called as disclinations.<sup>40</sup>

Interestingly, the conductivity of all composites is higher in the Col<sub>h</sub> mesophase compared to that in isotropic phase which is important from application point of view. The aligned sample provides a facile electron transport route as compared to unaligned sample.

A significant parameter of conductors formed by particle doped insulators is the frequency dependence of

conductivity. Jonscher's Universal Response is used to define frequency dependent conductivity in such type of materials including polymers, glasses, organic-inorganic composites etc.<sup>41</sup> At low frequencies, random diffusion of the ionic charge carriers via activated hopping gives rise to a frequency-independent conductivity. Whereas, at higher frequencies conductivity increases in a power-law fashion roughly exhibiting dispersion. So, total conductivity  $\sigma(f)$  measured at a finite frequency  $f$  is expressed as:

$$\sigma(f) = \sigma_{DC} + \sigma_{AC} \quad (1)$$

where,  $\sigma_{DC}$  and  $\sigma_{AC}$  are the DC component and AC contributions to conductivity. The Jonscher's universal description considers a distribution of hopping probabilities between sites distributed randomly in

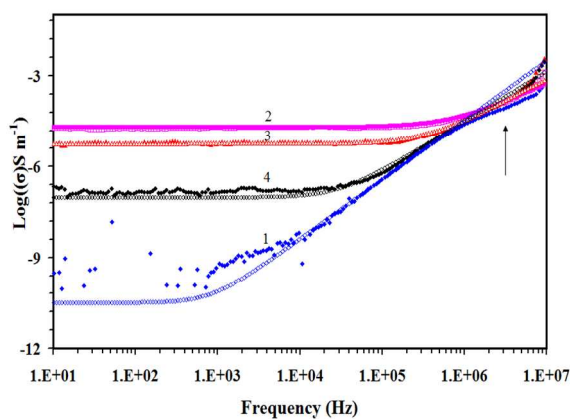


Figure 5: Frequency dependence of total conductivity ( $\sigma$ ), curve (1) Pure RTAQ (2) 0.5QDAQ (3) 1QDAQ and (4) 5QDAQ at 49.0°C. The open symbols represent the fit to eqn. 2. Arrow indicates a slight deviation from eqn. 2 due to presence of relaxation mode in this frequency region.

space and in energy. The expression used for  $\sigma(f)$  by Jonscher's universal description is:

$$\sigma(f) = \sigma_{DC}(1 + k(f/f_c)^n) \quad (2)$$

where,  $k$  and  $n$  are constants, ( $0 < n < 1$ ) for disordered solids. The onset of conductivity relaxation and the transformations from long range hopping to short range motions is marked by the critical frequency ( $f_c$ ). Fig. 5 represents variation of  $\log(\sigma)$  with frequency for pure and composites. The experimental data fit well with equation 2 except for pure because the conductivity measurements are not within the range of the used bridge. The critical frequency for all composites viz, 0.5QDAQ, 1QDAQ and 5QDAQ are 236.07 kHz, 137.54 kHz and 42.23 kHz respectively which are higher than that of the pure material (6.6 kHz). This indicates that QDs extend the long range hopping to a wider frequency range. The value of  $n$  as obtained by fitting for pure and composites are 1.96, 1.25, 1.44 and 1.65 respectively. The value of  $n$  is not between 0 and 1 as predicted by Jonscher. Papathanassiou *et al.* have proposed a model stating that there is no physical argument

to restrict the value of  $n$  below 1.<sup>42</sup> According to the authors, there does not exist a 'universal fractional power law'. They found lot of inefficiencies about the validity of the universal power law such as  $n$  is frequency dependent,  $n$  is greater than 1 for glassy  $0.3(x\text{Li}_2\text{O} \cdot (1-x)\text{Li}_2\text{O}) \cdot 0.7\text{B}_2\text{O}_3$  etc.<sup>43</sup> Recently, Prasad *et al.* have found some surprising results in liquid crystal gold nanocomposites formed by a gel network of aerosol particles.<sup>44</sup> The value of  $n$  for pure LC obtained by them was 1.95. The authors further averred that addition of nanoparticles in LCs reduces the value of the exponent  $n$  to such an extent that composite has values which are within the Jonscher's limit.<sup>44</sup>

The temperature dependent permittivity ( $\epsilon'$ ) plots for pure RTAQ and its three composites determined at a fixed frequency of 100 kHz are shown in fig 6. All the plots show an abrupt jump in the value of the

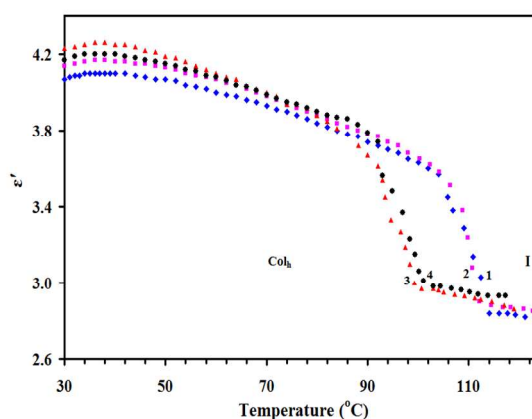


Figure 6: Thermal variation of permittivity ( $\epsilon'$ ) in isotropic and  $\text{Col}_h$  phases measured at 100 kHz for pure(1), 0.5QDAQ (2), 1QDAQ (3), and 5QDAQ (4). In each case there is a step change at the transition between the phases.

permittivity at the I- $\text{Col}_h$  transition. The value of permittivity in isotropic phase increases with increase in concentration of QDs. This feature suggests that there is an additional dipolar contribution from the semiconducting nanoparticles to the total permittivity of the medium. CdSe QDs possess a dipole moment.<sup>45</sup> The creation of an increased number of QD-DLC-QD capacitors may lead to the increase in permittivity of the composites. However, in liquid crystalline materials, increment in  $\epsilon'$  is associated with increase in orientational ordering. But in our case, results are contradictory. Increasing the concentration of QDs in the columnar matrix causes the decrease in the order of DLC as confirmed by conductivity studies. So, polarisability of QDs can be the valid reason for the enhancement in  $\epsilon'$ . At low temperatures, decrement in  $\epsilon'$  is seen for pure as well as composites. This is due to lowering of relaxation frequency so much so that frequency of measurement lies in dispersion region to be discussed subsequently.

Figure 7 shows the spectra for the real ( $\epsilon'$ ) and imaginary ( $\epsilon''$ ) parts of permittivity for pure DLC at various temperatures. It demonstrates that the DLC used

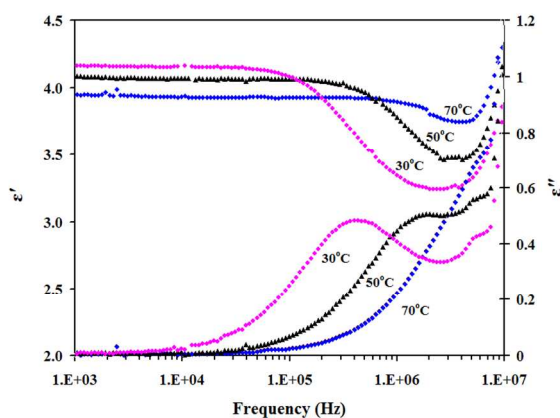


Figure 7: Variation of permittivity ( $\epsilon'$ ) and loss ( $\epsilon''$ ) with frequency for pure RTAQ

here has high value of permittivity than other discotics. Each RTAQ molecule is composed of two hydrogen bonds which provide stability to the mesophase. The data were processed by fitting the Cole-Cole equation<sup>46</sup> because there is very good evidence of the dielectric spectrum of Cole-Cole type (see figure 9):

$$\begin{aligned} \epsilon^* &= \epsilon' - j\epsilon'' \\ &= \epsilon'(\infty) + \sum \frac{\delta\epsilon}{1 + (j\omega\tau)^{(1-\alpha)}} + \frac{A}{\omega^n} - j \frac{\sigma_{DC}}{\epsilon_0\omega^k} - jB\omega^m \end{aligned} \quad (3)$$

where,  $\delta\epsilon = \epsilon(0) - \epsilon(\infty)$  is the dielectric strength of relaxation mode with  $\epsilon(0)$  and  $\epsilon(\infty)$  being the low and high frequency limiting values of the relative permittivity and  $\tau$  is the relaxation time. The parameter  $\alpha$  corresponds to symmetric distribution of the relaxation times with value in the range ( $0 < \alpha < 1$ ). The third and fourth terms in R.H.S of Equation (3) represent the contribution of the electrode polarization capacitance and DC conductivity at low frequencies. The fifth imaginary term  $B\omega^m$  is included in Equation (3) to partially account for the finite sheet resistance of ITO coated glass sheets used. A prominent dielectric relaxation is clearly visible in the 340 kHz-2 MHz region in Col<sub>h</sub> phase only which starts appearing at 74°C. It is important to note relaxation frequency ( $f_R$ ) of the mode lies approximately at the midpoint of the step of  $\epsilon'$  (i.e. point of inflexion) which corresponds to the peak point of  $\epsilon''$  data (see fig. 7).  $f_R$  decreases (due to the increase of viscosity which opposes the motions of the molecules) while  $\delta\epsilon$  increases (due to the improvement of the alignment) with decrease in temperature (refer fig. 7). The temperature dependence of  $f_R$  follows Arrhenius equation (fig 8):

$$f_R = A \exp\left(\frac{-E_A}{RT}\right) \quad (4)$$

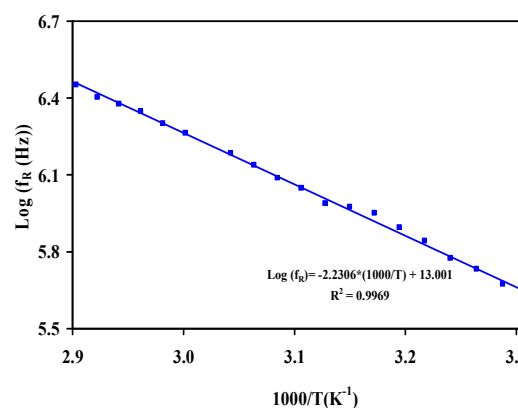


Figure 8: Temperature dependence of relaxation frequency for pure RTAQ following Arrhenius behavior.

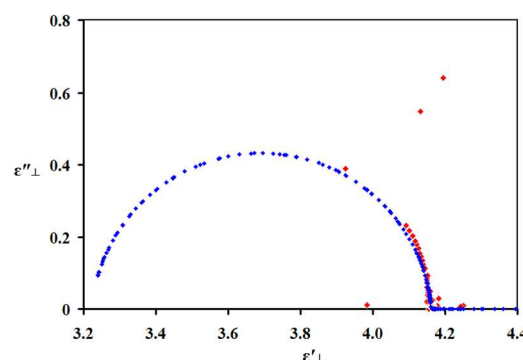


Figure 9: Cole-Cole plots showing the variation of the dielectric loss with relative permittivity for the pure.

where  $E_A$  denotes activation energy and  $R$  is ideal gas constant. The activation energy is estimated to be 42.67 kJ mol<sup>-1</sup>. It is elucidated that the observed relaxation is a Debye process from the value of distribution parameter  $\alpha = 0.06$  obtained by fitting experimental data as well as the Cole-Cole plot (fig. 9). The composites also repeat the same features as of the pure (refer fig. 10) but with appreciable changes in  $f_R$  and  $\delta\epsilon$  (see table 1). Table 1 show that  $f_R$  decreases with increase in the concentration of QDs. With the increasing concentration of QDs,  $\delta\epsilon$  is almost constant for RTAQ, 0.5QDAQ and 1QDAQ but it has appreciably decreased in the case of 5QDAQ (see table 1).

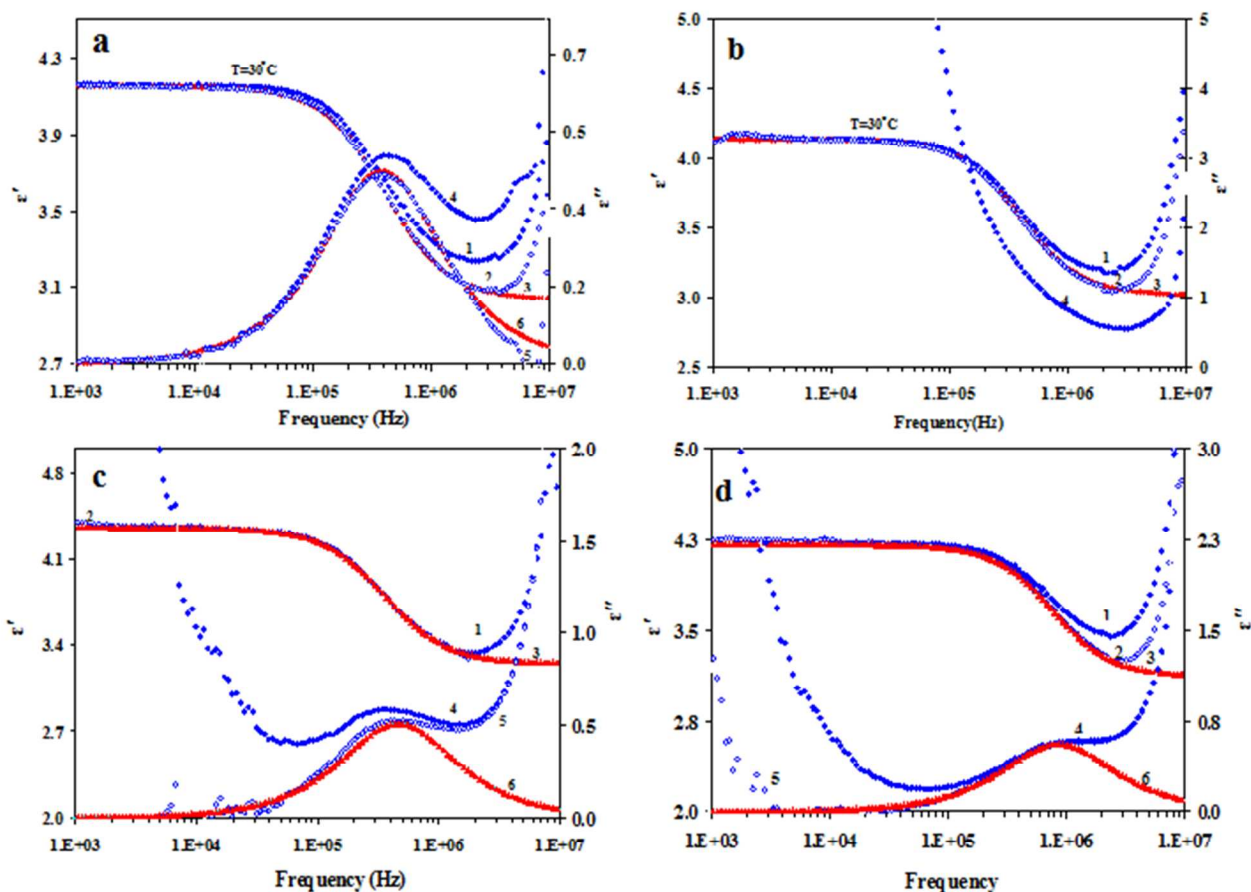
For other DLCs a similar relaxation process is observed. A value of 23 kJ mol<sup>-1</sup> was found for the  $E_A$  of relaxation in triphenylene derivate with five CH<sub>2</sub> groups.<sup>47</sup> For a pyrene derivative relatively low value of 10 kJ mol<sup>-1</sup> was reported.<sup>48</sup> The authors assigned it to localized fluctuations of the methylene groups. Discotic liquid crystalline hexabenzocoronene derivatives have activation energy of 50 kJ mol<sup>-1</sup>.<sup>49</sup> Such obtained values of activation energy are comparable to that identified for localized molecular motions perceived in polyethylene.<sup>50</sup> Hence, it is reasonable to accept that the relaxation mode observed here is arising due to local fluctuations of side chains of discotic molecules. Decrease of  $f_R$  is due to the increase in

the concentration of QDs as QDs (trapped between chains) increase inertia of the fluctuating chains. Further, due to the better packing, as free space for the movement of chains decreases, relaxation frequency decreases. However, in the case of 5QDAQ, one can notice marginal increase in the relaxation frequency. It has happened due to the dominating additional free space developed due to the heavy aggregation of QDs.

With the increasing concentration of QDs,  $\delta\epsilon$  is almost constant for RTAQ, 0.5QDAQ and 1QDAQ (slight decrease in this case, although within error of measurement) but it has appreciably decreased in the case of 5QDAQ. Later has occurred due to the disorder produced in the system due to the aggregation of QDs between the flexible chains (and hence poor alignment of the molecules) as discussed in previous sections. It is imperative to say that no such kind of relaxation has been reported earlier in anthraquinone derivatives.

### 3.4. SAXS studies

X-ray diffraction studies were performed in order to investigate the mesophase structure of the dispersed samples. A typical diffraction pattern is shown in fig 11 for 0.5QDAQ. Here, in the small angle region, two sharp peaks, one strong and other weak reflection can be seen whose d-spacings are in the ratio of 1:  $1/\sqrt{3}$  as in the case of RTAQ. This suggests that the two-dimensional hexagonal lattice structure of RTAQ is not disturbed due to addition of QDs. In the wide angle region, the broad peak corresponds to that of alkyl chains and another sharp peak shows the reflection due to (01) plane corresponding to core-core separation. X-Ray studies confirm that the composites also show columnar hexagonal phase. For pure material, intercolumnar distance is 22.4 Å and core-core



35

Figure 10: Dielectric relaxation spectra in Col<sub>h</sub> phase exhibiting a prominent relaxation process in real ( $\epsilon'$ ) and imaginary ( $\epsilon''$ ) components of permittivity. Curves 1 and 4 shows the measured value of  $\epsilon'$  and  $\epsilon''$ . Curve 3 and 6 shows the generated data for  $\epsilon'$  and  $\epsilon''$  by fitting to eqn. 3. Curve 2 and 5 represents the corrected data of  $\epsilon'$  and  $\epsilon''$  obtained after subtracting low and high frequency parasitic effects from the measured data. (a) Pure RTAQ (b) 0.5QDAQ, (c) 1QDAQ, and (d) 5QDAQ. In case of 0.5QDAQ, relaxation mode is not seen in loss data due to high conductivity.

Cite this: DOI: 10.1039/c0xx00000x

www.rsc.org/xxxxxx

## ARTICLE TYPE

Table 2: Inter-columnar distance ( $d_{\text{inter}}$  in Å) and average stacking distance (core-core separation in Å) of composites derived from diffraction patterns at different temperatures.

System	T (°C)	d-spacing (Å)	$d_{\text{inter}}$	core-core separation
0.5QDAQ	105	19.703	22.752	3.428
	80	19.588	22.612	3.381
	60	19.588	22.612	3.374
1QDAQ	105	19.782	22.843	-
	85	19.900	22.979	3.397
	70	19.900	22.979	3.377
5QDAQ	105	19.782	22.843	-
	85	19.900	22.979	3.407
	70	19.781	22.842	3.380

separation is 3.43 Å at 25.0°C.<sup>51</sup> QDs being 3.5nm in size easily embed themselves between columns, increasing the intercolumnar distances slightly. The average stacking distance (core-core separation) decreases to 3.38 Å for 0.5 wt% QD at 80.0°C. The decrease in core-core separation leads to better overlap between  $\pi$  orbitals, increasing conductivity in case of 0.5QDAQ. However, once the concentration of QDs is increased above 0.5 wt%, probably onset of aggregation of QDs minimizes the packing effects and the lattice tends to relax back to values of pure host material. For all the composites the core-core

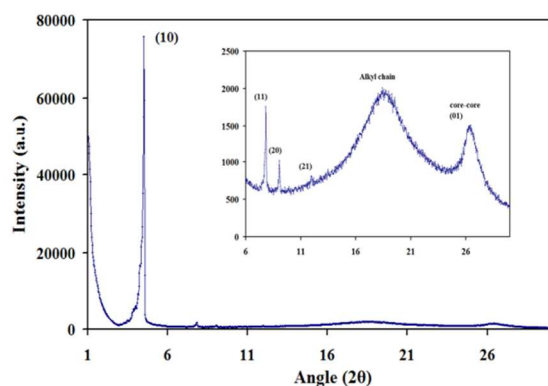


Figure 11: 1-Dimensional intensity versus  $2\theta$  profile for 0.5QDAQ composite. Inset shows enlarged view to show peaks of low intensity at 60.0°C.

separation decreases as temperature decreases (refer table 2). At 105.0°C, core-core separation could not be calculated because the peak was not discernable due to the sample being in isotropic phase for 5QDAQ.

#### 4. Conclusion

This journal is © The Royal Society of Chemistry [year]

The effect of dispersion of CdSe QDs on RTAQ shows that dispersion at low concentrations is uniform but at higher concentration shows aggregation. For low concentration when dispersion is uniform, stability of the columnar mesophase has enhanced. However, for high concentrations, when QDs tend to aggregate, stability of the mesophase decreases. Conductivity is enhanced by five orders of magnitude in the case of lowest concentration of QDs (i.e. 0.5 wt %) doped in RTAQ. For higher concentrations, conductivity enhancement is poor. Jonscher's universal response principle has been used to determine the critical frequency above which the conductivity becomes frequency dependent. The critical frequency has been found to be high for the composites suggesting that QDs enlarge the long range hopping. Dielectric spectroscopy of RTAQ shows a relaxation mode in the frequency range of few hundreds of kHz-MHz which arises due to local fluctuations of side chains of the discotic molecules, the first of its kind found in anthraquinone derivatives. The dynamics of the system as measured using the relaxation mechanism is seen to become slower in the presence of QDs. On the basis of these studies it is concluded that low concentration of QDs in pure DLC with uniform dispersion may be advantageous in bulk heterojunction as well as dye sensitized solar cells.

#### 5. Acknowledgements

This work is financially supported by Department of Electronics and Information Technology (DEITY) under a research project no. 12(6)/2011-EMCD. One of us (NY) thanks DEITY for fellowship under the project.

#### 6. References

1. S. Kumar, *Chemistry of Discotic Liquid Crystals: From Monomers to Polymers*, CRC Press, Boca Raton, FL, 2011.
2. V. Percec, M. Glodde, T. K. Bera, Y. Miura, I. Shiyonovskaya, K. D. Singer, V. S. K. Balagurusamy, P. A. Heiney, I. Schnell, A. Rapp, H.W. Spiess, S. D. Hudson and H. Duank, *Nature*, 2002, **419**, 384-387.
3. C. Grigoriadis, N. Haase, H. J. Butt, K. Mullen and G. Floudas, *Adv. Mater.*, 2010, **22**, 1403.
4. S. Kumar, *Chem. Soc. Rev.*, 2006, **35**, 83-109.
5. J. Billard, Z. Luz, R. Poupko and H. Zimmermann, *Liq. Cryst.*, 1994, **16**, 333-342.
6. K. S. Raja and S. Ramakrishnan, *Chem. Mater.*, 1997, **9**, 1630-1637.

7. H. Iino, Y. Takayashiki and J. Hanna, *Appl. Phys. Lett.*, 2005, **87**, 192105-1-3.
8. Y. D. Zhang, K. G. Jespersen, M. Kempe, J. A. Kornfield, S. Barlow, B. Kippelen and S. R. Marder, *Langmuir*, 2003, **19**, 6534-6536.
9. B. R. Acharya, H. Choi, M. Srinivasarao and S. Kumar, *Appl. Phys. Lett.*, 2011, **99**, 221108.
10. J. Eccher, G. C. Faria, H. Bock, H.V. Seggern and I. H. Bechtold, *ACS Appl. Mater. Interfaces*, 2013, **5**, 11935-11943.
11. N. Boden, R. C. Bomer, R. J. Bushby and J. Clements, *J. Am. Chem. Soc.* 1994, **116**, 10807-10808.
12. L. E. Brus, *J. Chem. Phys.*, 1984, **80**, 4403-4409.
13. A. Mandal, J. Nakayama, N. Tamai, V. Biju and M. Isikawa, *J. Phys. Chem. B*, 2007, **111**, 12765-12771.
14. L. Chen, J. D. Lin and C. R. Lee, *J. Mater. Chem. C*, 2014, **2**, 4388-4394.
15. K. A. Piegdon, M. Offer, A. Lorke, M. Urbanski, A. Hoischen, H. S. Kitzerow, S. Declair, J. Forstner, T. Meier, D. Reuter, A. D. Wieck and C. Meier, *Physica E*, 2010, **42**, 2552-2555.
16. I. Gur, N. A. Fromer, M. L. Geier and P. Alivisatos, *Science*, 2005, **310**, 462-464.
17. R. S. Selinsky, Q. Ding, M. S. Faber, J. C. Wright and S. Jin, *Chem. Soc. Rev.*, 2013, **42**, 2963-2985.
18. M. Kumar and S. Kumar, *RSC Adv.*, 2015, **5**, 1262-1267.
19. R. Basu and G. S. Iannacchione, *Phys. Rev. E*, 2009, **80**, 010701.
20. A. Kumar and A. M. Biradar, *Phys. Rev. E*, 2011, **83**, 041708.
21. J. Mirzaei, M. Reznikov and T. Hegmann *J. Mater. Chem.*, 2012, **22**, 22350-22365.
22. B. Kinkead and T. Hegmann, *J. Mater. Chem.*, 2010, **20**, 448-458.
23. H.K. Bisoyi and S. Kumar, *Tetrahedron Lett.*, 2007, **48**, 4399-4402.
24. S. Kumar and L. Sagar, *Chem. Commun.*, 2011, **47**, 12182.
25. U. B. Singh, R Dhar, A. S. Pandey, S. Kumar, R. Dabrowski and M. B. Pandey, *AIP Adv.*, 2014, **4**, 117112.
26. M. Mishra, S. Kumar and R. Dhar, *RSC. Adv.* 2014, **4**, 62404-62412.
27. N. Yadav, R. Dabrowski and R. Dhar, *Liq. Cryst.*, 2014, **41**, 1803-1810.
28. R. Dhar, R.S. Pandey and V.K. Agarwal, *Ind. J. Pure Appl. Phys.*, 2002, **40**, 901-907.
29. A. Dwivedi, R. Dhar and R. Dabrowski, *Soft Materials*, 2009, **7**, 54-65.
30. M. V. Gorkunov, G. A. Shandryuk, A. M. Shatalova, I. Y. Kutergina, A. S. Merkalov, Y. V. Kudryavtsev, R. V. Talroze and M. A. Osipov, *Soft Matter*, 2013, **9**, 3578-3588.
31. H. Bengs, F. Closs, T. Frey, D. Funhoff, H. Ringsdorf and K. Siemensmeyer, *Liq. Cryst.*, 1993, **15**, 565-574.
32. V. Prasad, K. Krishnan and V.S.K. Balagurusamy, *Liq. Cryst.*, 2000, **27**, 1075-1085.
33. E. Fontes and P. A. Heiney, *Phys. Rev. A*, 1988, **37**, 1329-1334.
34. X. Feng, L. S. Vargas, S. Umadevi, T. Mori, Y. Shimizu and T. Hegmann, *Adv. Funct. Mater.*, 2014, DOI: 10.1002/adfm.201401844.
35. V. Lemaure, D. A. da Silva Filho, V. Coropceanu, M. Lehmann, Y. Geerts, J. Piris, M. G. Debije, A. M. van de Craats, K. Senthilkumar, L. D. A. Siebbeles, J. M. Warman, J.-L. Bredas and J. Cornil, *J. Am. Chem. Soc.*, 2004, **126**, 3271-3279.
36. M. Lehmann, G. Kestemont, R. G. Aspe, C. B. Herman, M. H. J. Koch, M. G. Debije, J. Piris, M. P. de Haas, J. M. Warman, M. D. Watson, V. Lemaure, J. Cornil, Y. H. Geerts, R. Gearba and D. A. Ivanov, *Chem. Eur. J.* 2005, **11**, 3349 - 3362.
37. S. Chandrasekhar and G. S. Ranganath, *Rep. Prog. Phys.*, 1990, **53**, 57-84.
38. M. Yoneya, T. Makabe, A. Miyamoto, Y. Shimizu, Y. Miyake, H. Yoshida, A. Fujii and M. Ozaki, *Phys. Rev. E*, 2014, **89**, 062505.
39. A. M. van de Craats, J. M. Warman, A. Fechtenkötter, J. D. Brand, M. A. Harbison and K. Mulen, *Adv. Mater.*, 1999, **11**, 1469.
40. T. A. Wood, J. S. Lintuvuori, A. B. Schofield, D. Marenduzzo and W. C. K. Poon, *Science*, 2011, **334**, 80-83.
41. A.K. Jonscher, *Nature*, 1977, **267**, 673.
42. A. N. Papatthanassiou, I. Sakellis and J. Grammatikakis, *Appl. Phys. Lett.* 2007, **91**, 122911.
43. C. Cramer, S. Brunklaus, E. Ratai and Y. Gao Y, *Phys. Rev. Lett.*, 2003, **91**, 266601.
44. B. Kamaliya, M.V. Kumar, C. V. Yelamaggad and S. K. Prasad, *Appl. Phys. Lett.* 2015, **106**, 083110.
45. S.A. Blanton, R.L. Leheny, M.A.Hines and P. Guyot-Sionnest, *Phy.Rev. Lett.* 1997, **79**, 865.
46. W. Hasse and S. Wrobel, *Relaxation Phenomena: Liquid Crystals, Magnetic Systems, Polymers, High Tc Superconductors, Metallic Glasses*, Springer -Verlag, Berlin Heidelberg, 2003.
47. Z. Yildirim, M. Wubbenhorst, E. Mendes, S. J. Picken, I. Paraschiv, A. T.M. Marcellis, H. Zuilhof and E. J.R. Sudholter, *J. Non-Cryst. Solids*, 2005, **351**, 2622-2628.
48. C. Krause, H. Yin, C. Cerclier, D. Morineau, A. Wurm, C. Schick, F. Emmerling and A. Schonhals, *Soft Matter*, 2012, **8**, 11115-11122.
49. A. Schonhals, H. Goering, F. R. Costa, U. Wagenknecht and G. Heinrich, *Macromolecules* 2009, **42**, 4165-4174.
50. O. Van den Berg, W.G.F. Sengers, W.F. Jager, S.J. Picken and M. Wubbenhorst, *Macromolecules*, 2004, **37**, 2460.
51. H.K. Bisoyi and S. Kumar, *New J. Chem.*, 2008, **32**, 1974-1980.